Theoretical CSPR Analysis and Performance Comparison for Four Single-Sideband Modulation Schemes With Kramers-Kronig Receiver

DONGXU LU[1], XIAN ZHOU[1], (Member, IEEE), JIAHAO HUO[1], JIE GAO[1], YUQIANG YANG[1], KE HE[1], JINHUI YUAN[1], (Senior Member, IEEE), KEPING LONG[1], (Senior Member, IEEE), CHANGYUAN YU[2], (Member, IEEE), ALAN PAK TAO LAU[3], (Member, IEEE), AND CHAO LU[2], (Senior Member, IEEE)

[1]Beijing Engineering and Technology Research Center for Convergence Networks and Ubiquitous Services, University of Science and Technology Beijing, Beijing 100083, China
[2]Photonics Research Centre, Department of Electronic and Information Engineering, The Hong Kong Polytechnic University, Hong Kong
[3]Photonics Research Centre, Department of Electrical Engineering, The Hong Kong Polytechnic University, Hong Kong

Corresponding authors: Xian Zhou (zhouxian219@ustb.edu.cn) and Ke He (heke@tsinghua-eiri.org)

ABSTRACT Recently, high-speed optical transmission using single-side-band (SSB) modulation with Kramers-Kronig (KK) scheme has gained great attention due to its high spectral efficiency (SE) and capability of electronic chromatic dispersion compensation (CDC), which can be widely employed in optical metro networks as a promising transmission scheme. To our knowledge, the carrier-signal power ratio (CSPR) is the key parameter to SSB-based systems and the optimum CSPRs can vary distinctly in different SSB modulation schemes. In this paper, the SSB-based KK systems with four kinds of SSB signal generation schemes are investigated, i.e. optical carrier-assisted SSB (OCA-SSB), virtual carrier-assisted SSB (VCA-SSB), SSB subcarrier modulation (SSB SCM) with IQ modulator (IQM) and with dual-drive Mach–Zehnder modulator (DDMZM) respectively. Here, the detailed theoretical derivations of these modulation processing are given and the theoretical relationship between device parameters and the CSPR has been further studied for the different SSB schemes. In order to verify those theoretical analyses, a 224-Gb/s direct detection (DD) transmission with SSB 16-ary quadrature amplitude modulation (16-QAM) signal has been demonstrated based on four SSB generation methods. The results show that theoretical derivations are closely consist with numerical analysis, such as V_{bias} in the scheme of SSB SCM with IQM and optical modulation index (OMI) in SSB SCM with DDMZM. Therefore, our research can provide a theoretical guidance of appropriate device parameter configuration so as to achieve the optimum performance for SSB systems.

INDEX TERMS Direct detection, single sideband, IQ modulator, DDMZM, Kramers-Kronig.

I. INTRODUCTION

To satisfy the ever-growing capacity demand for cloud service and data-center interconnect (DCI) applications, short-reach optical communication based on direct detection (DD)

The associate editor coordinating the review of this manuscript and approving it for publication was San-Liang Lee.

has drawn more and more attention recently [1]. For such scenarios, the cost-effectiveness is the crucial requirement combined with low power consumption. To achieve this, the system complexity of optical transmission architecture needs to be relatively simple with low-cost and low-complexity components. In comparison with coherent detection, DD systems using only one single-ended

photodiode and one analogue-to-digital converter (ADC) are potentially more preferable for optical access/metro network and data center interconnecting due to its simpler system structure and significant lower system cost [2].

During recent years, various advanced modulation formats have been investigated to achieve high spectral efficiency (SE) in DD systems [3]–[6], such as discrete multi-tone (DMT) [7]–[9], carrier-less amplitude and phase (CAP) modulation [10]–[12], quadrature amplitude modulation (QAM) [13]–[16], subcarrier modulation (SCM) [17]–[19], and pulse-amplitude modulation (PAM) [20]–[22]. Besides, single-side-band (SSB) modulation is becoming a promising scheme because of its improvement of the SE and resistance to chromatic dispersion. In general, several ways for generating SSB signal can be summarized into four categories in terms of the different signal filtering schemes (using the optical filter [23], [24] or digital filter [25]–[27]) and different carrier addition methods (adding the optical carrier [28], [29] or digital carrier [30]–[32]). The first approach is widely regarded as a straightforward technique, which uses an optical band-pass filter (OBPF) to remove one sideband from the double sideband (DSB) signal in the optical field. Except the additional cost of optical filter, when the spectrum gap between the carrier and SSB signal becomes narrow, the sideband supposed to be removed will have some residual due to the non-ideal optical filter characteristics. Unlike the first approach, a digital SSB filter based on Hilbert transformation is adopted at the transmitter (Tx) of the second approach, the representative of which is regarded as SSB SCM scheme in the recent research [33], [34]. This scheme employs an in-phase quadrature modulator (IQM) or dual-drive Mach–Zehnder modulator (DDMZM) to map SSB digital signal linearly into the optical field [35]. The third approach with an optical carrier added to the edge of signal spectrum can generate an optical carrier-assisted SSB (OCA-SSB) signal [28]. The last approach generates a digital tone acting as a virtual carrier together with the transmitted signal at the Tx [36], which is named the virtual carrier-assisted single sideband (VCA-SSB) method in this paper.

However, the SSB DD system still has an obvious drawback to degrade system performance, which is the signal-signal beat interference (SSBI) introduced by photodetector (PD) square-law detection. Several SSBI cancellation techniques have been extensively proposed, such as the single-stage linearization filter, the iterative linearization filter, the two-stage linearization filter, the SSBI estimation and cancellation technique and the Kramers-Kronig (KK) scheme [37]–[42]. Among these SSBI cancellation techniques, KK scheme is considered as the best solution of SSBI migration techniques in Ref. [43], which has smaller carrier-signal power ratio (CSPR) and lower digital signal processing (DSP) algorithm complexity compared with the other techniques. The most outstanding character of KK scheme is that the signal's phase can be exactly reconstructed from the detected amplitude waveform through

the KK relation, when the carrier added to the edge of information-carrying signal spectrum is large enough to satisfy the minimum phase (MP) condition [44].

In this paper, four kinds of SSB generation schemes combined with KK receiver have been investigated, which are OCA-SSB, VCA-SSB, SSB SCM with IQM and SSB SCM with DDMZM respectively. Based on the transfer function of modulator and SSB modulation principles, theoretical derivations of different modulation processing and the relationship between the modulator parameters of the CSPR are proposed. In particular, the calculation formulas of CSPRs in four SSB systems are summarized. To verity the theoretical analysis, a transmission with 224-Gb/s SSB 16-QAM signal has been demonstrated on a unified optical system platform, in which the BER performance versus the CSPR and optical signal-to-noise ratio (OSNR) is given with detailed analyses. The results show that the theoretical derivations are in good agreement with simulation numerical analyses.

The rest of the paper is organized as follows. Section II gives theoretical derivations of the modulation processing, numerical analyses of the CSPR and relation between OSNR and BER under different CSPRs. Section III presents the DSP algorithms of the system simulation setup and the main parameters of devices. In Section IV, parametric optimizations and evaluation of BER performance for four systems are provided under different DSP configurations with the explanation correspondingly. Finally, we summarize this work.

II. THEORETICAL ANALYSES OF SSB DD SYSTEMS

Fig. 1 shows four implementation diagrams of SSB DD systems along with illustrations for the spectrum of SSB signal, namely, (a) OCA-SSB, (b) VCA-SSB, (c) SSB SCM with IQM and (d) SSB SCM with DDMZM. For simplicity, the frequency of the added carrier offset in (a) and (b) and subcarrier in (c) and (d) are set to be half of the bandwidth of baseband signal ($B/2$). Next, the relationship between BER, OSNR and CSPR theoretically for SSB signals is given.

A. PRINCIPLE OF GENERATING SSB SIGNAL

At first, theoretical derivations of modulation processing and CSPRs are given in detail based on four SSB schemes.

1) OCA-SSB WITH IQ MODULATOR

Based on the transfer function of IQ modulator and SSB modulation principles, when the extinction ratio (ER) is ideal and the insert loss of modulator is neglected, the output of IQM can be expressed as [45]

$$
\begin{aligned}
E_{\text{out}}(t) = \ &\frac{1}{2}E_{in}(t)\left[\frac{1}{2}\exp\left(j\frac{\pi}{V_\pi}(V_I + V_{Ibias})\right)\right.\\
&\left. + \frac{1}{2}\exp\left(-j\frac{\pi}{V_\pi}(V_I + V_{Ibias})\right)\right]\\
&+ \frac{1}{2}E_{in}(t)\left[\frac{1}{2}\exp\left(j\frac{\pi}{V_\pi}(V_Q + V_{Qbias})\right)\right.\\
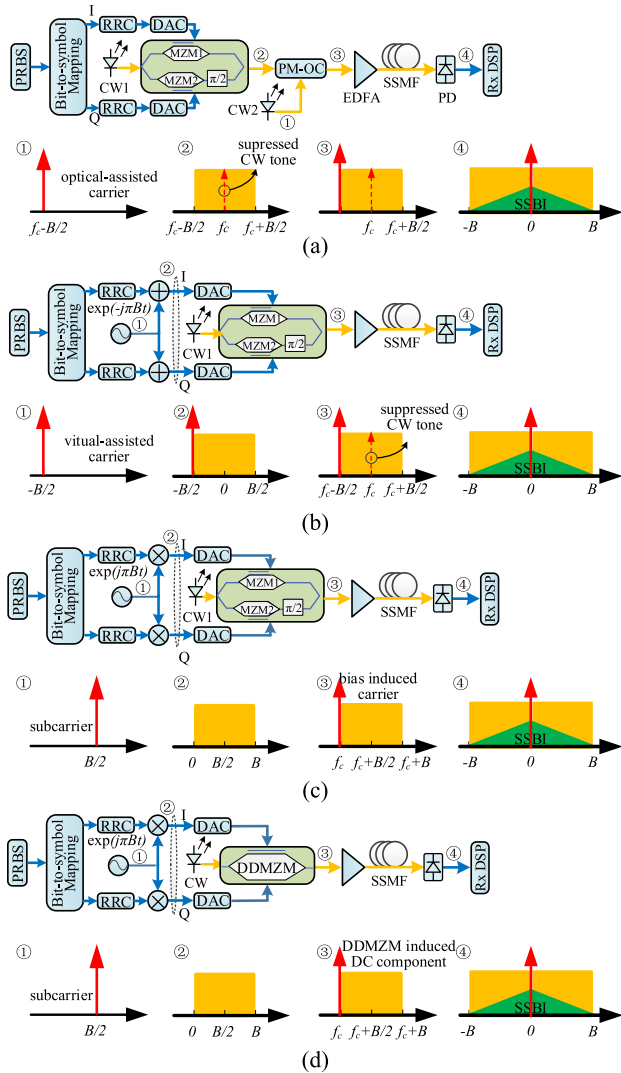&\left. + \frac{1}{2}\exp\left(-j\frac{\pi}{V_\pi}(V_Q + V_{Qbias})\right)\right]
\end{aligned}
$$

FIGURE 1. Different SSB generation techniques. (a) OCA-SSB. (b)VCA-SSB. (c) SSB SCM with IQ modulator. (d) SSB SCM with DDMZM.

$$= \frac{1}{2} E_{in}(t) \left[\cos\left(\frac{\pi}{V_\pi}(V_I + V_{Ibias}) \right) + j\cos\left(\frac{\pi}{V_\pi}(V_Q + V_{Qbias}) \right) \right] \quad (1)$$

where $E_{in}(t)$ is the input optical field, $E_{out}(t)$ is the output optical field, V_{Ibias} and V_{Qbias} are the DC bias voltage of two parallel phase modulators (I and Q branches), V_π is the half-voltage of the two electrodes, and V_I and V_Q are two electrical signals to drive the modulators.

By setting $V_{Ibias} = V_{QBias} = -V_\pi/2$ and assuming a low-amplitude signal, Eq. (1) can be written as

$$E_{out}(t) = \frac{E_{in}(t)}{2} \left[\sin(\frac{\pi}{V_\pi} V_I) + j\sin\left(\frac{\pi}{V_\pi} V_Q \right) \right]$$
$$\approx \frac{E_{in}(t)}{2} \frac{\pi}{V_\pi} \underbrace{(V_I + jV_Q)}_{\text{TX signal}} \quad (2)$$
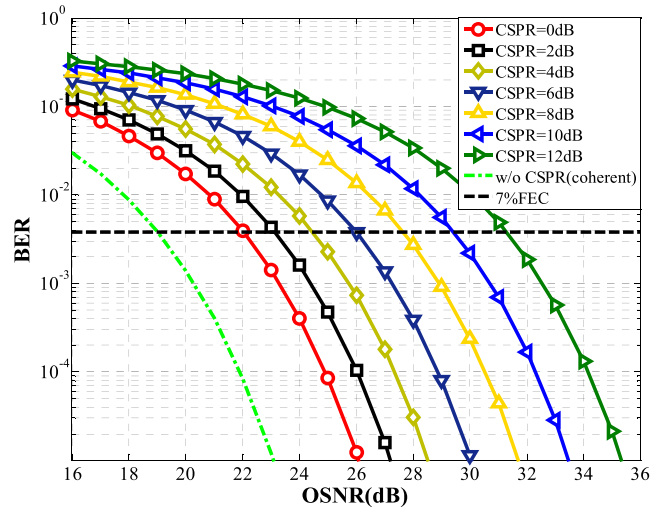

FIGURE 2. Theoretical BER versus OSNR for 56 GBaud 16-QAM system under different CSPRs.

where the Tx signal represents the output signal of the transmitter. As is demonstrated in Fig. 1(a), the I/Q modulator is biased at the null-point to suppress the optical carrier in the OCA-SSB system. The optical SSB signal can be generated by using an IQM with an additional optical tone appended to the signal spectrum at the frequency of $-B/2$ and using a polarization-maintaining optical coupler (PM-OC) to align the polarization of carrier and signal at the transmitter side. The extra optical carrier can be produced by an additional laser or the optical frequency comb generation (OFCG), which increases the cost in terms of system implementation. In this scheme, the optical SSB signal and CSPR can be written as

$$S_{\text{out}}(t) = \left[E_{out}(t) + A_1 \exp\left(j2\pi(-\frac{B}{2})t \right) \right] \exp(j2\pi f_c t) \quad (3)$$

$$CSPR_1 = 10 \log_{10} \frac{P_{carrier}}{P_{signal}} = 10 \log_{10} \frac{A_1^2}{|E_{out}(t)|^2}$$
$$= 10 \log_{10} \left(\frac{4V_\pi^2 A_1^2}{\pi^2 |E_{in}(t) \cdot s(t)|^2} \right) \quad (4)$$

where f_c is the center frequency of CW1 in Fig. 2(a), A_1 is the amplitude of the optical carrier generated by CW2 and $s(t)$ is the baseband signal of bit-to-symbol mapping at a bandwidth of B. In this model, the Tx signal and $s(t)$ share the same meaning.

2) VCA-SSB WITH IQ MODULATOR

Fig. 2(b), that is VCA-SSB, detailedly depicts a simple but practical SSB system structure by adding a digital tone as a virtual carrier together with the transmitted signal at the Tx, which also employs only two DACs and one IQ modulator (the same to OCA-SSB). Different from the first method, the Tx signal of this scheme is written as $s(t) + A\exp(j2\pi(B/2)t)$. The output of IQM and CSPR can be

expressed as

$$E_{out}(t) = \frac{E_{in}(t)}{2} \frac{\pi}{V_\pi} \left[s(t) + A_2 \exp\left(j2\pi(-\frac{B}{2})t \right) \right] \exp(j2\pi f_c t) \tag{5}$$

$$CSPR_2 = 10\log_{10} \frac{P_{carrier}}{P_{signal}} = 10\log_{10} \frac{A_2^2}{|s(t)|^2} \tag{6}$$

where A_2 is the amplitude of the virtual carrier. By comparing Eq. (4) and Eq. (6), we can draw a conclusion that $CSPR_1$ can be influenced by not only the signal power, optical carrier power and V_π but also the input laser power, yet $CSPR_2$ is only in relation to the former two factors.

3) SSB SCM WITH IQ MODULATOR

The SSB Nyquist pulse-shaped SCM schemes, also referred as SSB SCM, can achieve the SSB generation by using an IQM or a DDMZM, which are demonstrated in Fig. 2(c) and Fig. 2(d) respectively. The two SSB Nyquist baseband signals are both up-converted to a subcarrier frequency (f_{sc}) of $B/2$ by multiplying $\exp(j2\pi(B/2)t)$. Rather than the null-point, the IQM or DDMZM is biased above or below the point to induce the optical carrier.

Besides, as shown in Fig. 2, it's worthy noted that the analog bandwidth of technique (c) and (d) is twice that of (a) and (b), because SSB SCM schemes transmit the SSB signal to cause half of the bandwidth not to be utilized while the carrier-assisted methods transmit the DSB signal at the Tx. To adopt the transfer function of IQ modulator in Eq. (1), the output of the SSB SCM with IQM can be written as

$$E_{out}(t) = \frac{E_{in}(t)}{2} \left[\cos\left(\frac{\pi}{V_\pi}(V_I + V_{Ibias}) \right) \right.$$
$$\left. + j\cos\left(\frac{\pi}{V_\pi}(V_Q + V_{Qbias}) \right) \right]$$
$$= \frac{E_{in}(t)}{2} \left[\cos\left(\frac{\pi}{V_\pi}V_I \right) \cos\left(\frac{V_{Ibias}}{V_\pi}\pi \right) - \sin\left(\frac{\pi}{V_\pi}V_I \right) \right.$$
$$\times \sin\left(\frac{V_{Ibias}}{V_\pi}\pi \right) + j\left(\cos\left(\frac{\pi}{V_\pi}V_Q \right) \cos\left(\frac{V_{Qbias}}{V_\pi}\pi \right) \right.$$
$$\left. \left. - \sin\left(\frac{\pi}{V_\pi}V_Q \right) \sin\left(\frac{V_{Qbias}}{V_\pi}\pi \right) \right) \right] \tag{7}$$

where the Tx signal of this SSB scheme can be expressed as $V_I + jV_Q = s(t)\exp(j2\pi(B/2)t)$. Assuming that the in-phase component V_I and quadrature component V_Q are low-amplitude values, thus high order terms can be negligible. Therefore, by setting $V_{Ibias} = V_{Qias} = V_{bias}$ the second-order Taylor series expansion of $E_{out}(t)$ is given by

$$E_{out}(t) = \frac{E_{in}(t)}{2} \left[\left(1 - \frac{1}{2}(\frac{\pi}{V_\pi}V_I)^2 \right) \cos\left(\frac{V_{bias}}{V_\pi}\pi \right) \right.$$
$$\left. - \left(\frac{\pi}{V_\pi}V_I \right) \sin\left(\frac{V_{bias}}{V_\pi}\pi \right) \right.$$

$$+ j\left((1 - \frac{1}{2}(\frac{\pi}{V_\pi}V_Q)^2) \cos\left(\frac{V_{bias}}{V_\pi}\pi \right) \right.$$
$$\left. - \left(\frac{\pi}{V_\pi}V_Q \right) \sin\left(\frac{V_{bias}}{V_\pi}\pi \right) \right) \right]$$
$$= \frac{E_{in}(t)}{2} \left[(1+j)\cos\left(\frac{V_{bias}}{V_\pi}\pi \right) - \frac{\pi}{V_\pi}(V_I + jV_Q)\sin \right.$$
$$\left. \times \left(\frac{V_{bias}}{V_\pi}\pi \right) - \frac{1}{2}(\frac{\pi}{V_\pi})^2(V_I^2 + jV_Q^2)\cos\left(\frac{V_{bias}}{V_\pi}\pi \right) \right] \tag{8}$$

According to Eq. (8), we can deduce the formula of CSPR in SSB SCM system with the IQM, which can be given by

$$CSPR_3 = 10\log_{10} \frac{P_{carrier}}{P_{signal}} = 10\log_{10} \frac{\left| (1+j)\cos\left(\frac{V_{bias}}{V_\pi}\pi \right) \right|^2}{\left| \frac{\pi}{V_\pi}\sin(\frac{V_{bias}}{V_\pi}\pi) \right|^2 \overline{|s(t)|^2}}$$
$$= 10\log_{10} \frac{2}{\left(\frac{\pi}{V_\pi} \right)^2 \tan^2\left(\frac{V_{bias}}{V_\pi}\pi \right) \overline{|s(t)|^2}} \tag{9}$$

4) SSB SCM WITH DDMZM

Similarly, a DDMZM consists of two phase modulators, driven by two independent electrical signals (V_I and V_Q), the DC bias voltage of which are V_{bias1} and V_{bias2} respectively. As is shown in Fig. 2(d), by setting $V_{bias2} - V_{bias1} = V_\pi/2$ and assuming that the ER condition is ideal and the signal is low-amplitude, the second-order Taylor series expansion of the DDMZM input–output relationship can be written as

$$E_{out}(t) = \frac{E_{in}(t)}{2} \left[\exp\left(j\frac{\pi}{V_\pi}(V_1 + V_{bias1}) \right) \right.$$
$$\left. + \exp\left(j\frac{\pi}{V_\pi}(V_2 + V_{bias2}) \right) \right]$$
$$= \frac{E_{in}(t)}{2} \left[\exp\left(j\frac{\pi}{V_\pi}(V_1 + V_{bias2} - \frac{V_\pi}{2}) \right) \right.$$
$$\left. + \exp\left(j\frac{\pi}{V_\pi}(V_2 + V_{bias2}) \right) \right]$$
$$\approx \frac{E_{in}(t)}{2} \left[-j\left(1 + j\frac{\pi}{V_\pi}V_1 - \frac{\pi^2}{V_\pi^2}V_1^2 \right) \exp(j\frac{\pi}{V_\pi}V_{bias2}) \right.$$
$$\left. + \left(1 + j\frac{\pi}{V_\pi}V_2 - \frac{\pi^2}{V_\pi^2}V_2^2 \right) \exp(j\frac{\pi}{V_\pi}V_{bias2}) \right]$$
$$= \frac{E_{in}(t)}{2} \exp(j\frac{\pi}{V_\pi}V_{bias2}) \left[(1-j) + \frac{\pi}{V_\pi}(V_1 + jV_2) \right.$$
$$\left. + \frac{\pi^2}{V_\pi^2}(jV_1^2 - V_2^2) \right] \tag{10}$$

According to Eq. (10), if adopted in the carrier addition method, the DDMZM can bring a large power penalty due to the large DC component, and hence the CSPR is more difficult to meet the MP condition in KK scheme. So the DDMZM is suitable for SSB SCM rather than the carrier-assisted SSB system. Besides, optical modulation index (OMI) is a common parameter to measure the performance of the DDMZM, which can be defined as $OMI = V_{RF}^{rms}/V_\pi$, V_{RF}^{rms} corresponds

to the root-mean-square (RMS) of the electrical input to the DDMZM. Therefore, the CSPR of SSB SCM with DDMZM method can be deduced as

$$CSPR_4 = 10 \log_{10} \frac{P_{carrier}}{P_{signal}} = 10 \log_{10} \frac{|1-j|^2}{\left(\frac{\pi}{V_\pi}\right)^2 \overline{|s(t)|^2}}$$

$$= 10 \log_{10} \frac{2}{\left(\frac{\pi}{V_\pi}\right)^2 \overline{|s(t)|^2}} = 10 \log_{10} \frac{2}{\pi^2 OMI^2} \quad (11)$$

Based on the conclusion of $CSPR_3$ and $CSPR_4$, we can find that the CSPR of SSB SCM with DDMZM is only related to V_π and the input electric signal and correspondingly the CSPR of SSB SCM with IQM is relevant to the bias voltage of IQM except the former two parameters.

B. THE RELATIONSHIP BETWEEN THE BER, OSNR AND CSPR THEORETICALLY

In this paper, when referring to the OSNR, the power of signal contains both the carrier and signal. For clear distinction, $OSNR_{equivalent}$ here means the effective OSNR, which contains the total signal power without the CW tone. Thus there is a certain relationship between $OSNR$, $OSNR_{equivalent}$ and $CSPR$, which can be expressed as [28]

$$OSNR = \frac{P_{signal} + P_{carrier}}{P_{noise}} = \frac{P_{signal}}{P_{noise}}(CSPR + 1)$$

$$= OSNR_{equivalent} \times (CSPR + 1)$$

$$= \frac{(CSPR + 1) \times E_b R_b}{2N_0 B_{ref}} \quad (12)$$

where E_b refers to the average power per bit of the signal in one polarization, R_b represents the bit rate, N_0 means the spectral density of the received amplified spontaneous emission (ASE) noise in each polarization and B_{ref} is the optical bandwidth reference usually set as 0.1 nm.

Besides, we can also give the theoretical BER conclusion of M-QAM signal

$$BER = \frac{4(\sqrt{M} - 1)}{\sqrt{M} \log_2 M} Q \left[\sqrt{\frac{3 \log_2 M}{M-1} \cdot \frac{E_b}{N_0}} \right] \quad (13)$$

To combine Eq. (12) and Eq. (13), we can get the relationship between the OSNR and BER under different CSPRs in theory. By setting the baud rate of 56 GBaud and increasing CSPR from 0 dB to 12 dB, Fig. 2 demonstrates the theoretical relationship between this three key system parameters on ideal conditions, in which Additive White Gaussian Noise (AWGN) is the only noise source considered and SSBI or other non-ideal system factors are not considered.

III. SIMULATION SETUP

The simulation setup and DSP block diagram are shown in Fig. 3 and the main parameters are summarized in Table 1. This is conducted by VPItransmissionMaker8.7 and Matlab.

At the transmitter, the data stream with a pseudo random bit sequence (PRBS) length of $2^{16}-1$ is mapped to 16-QAM symbols. Next 56 Gbaud 16-QAM symbols are
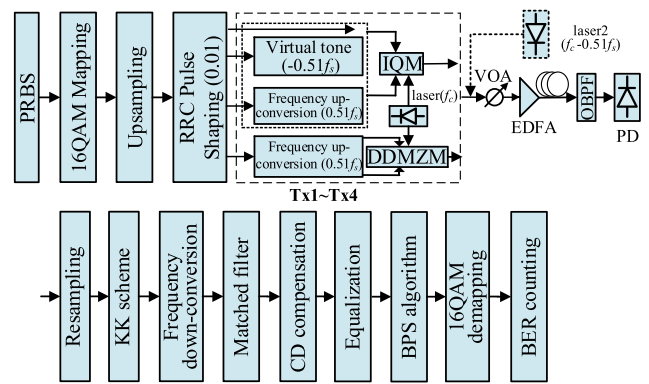
FIGURE 3. Simulation setup and DSP of four SSB DD methods with 56 GBaud 16QAM signal.

TABLE 1. General simulation parameters of 224Gbit/s SSB dd systems.

Parameter	Value
Baud rate	56 Gbaud
DAC/ADC sampling rate	112 GSa/s
The ENOB of DAC/ADC	6 bits
Laser linewidth	100 kHz
Laser Power	15 dBm
V_π(IQM&DDMZM)	3 V
Extinction Ratio (IQM & DDMZM)	30dB & 25dB
Noise figure of EDFA	5dB
Chromatic dispersion	17 ps/nm/km
PD responsibility	0.65 A/W
PD thermal noise	20 pA/Hz$^{0.5}$
PD dark current	10 nA

8 times up-sampled and digitally shaped using a root raise cosine (RRC) filter with a roll-off factor of 0.01. For the Tx1 (OCA-SSB), the real and imaginary parts are fed into the IQM directly, which is biased at its null-point to suppress the optical carrier. And for the Tx2, a RF tone with the frequency of 28.56 GHz ($0.51\times$ symbol rate (f_s)) is added, which locates at the left edge of the signal band. In this case, the IQM is also biased at its null-point. For the T $\times$ 3 and T $\times$ 4, the baseband 16-QAM Nyquist signal is frequency up-converted by multiplexing, where the subcarrier frequency is also $0.51\times$ symbol rate. Different from the first two methods, SSB SCM with IQM offset the IQ modulator bias to generate an optical carrier at the optical frequency of the transmitter laser. For Tx4, according to Eq. (10), the DDMZM is biased at the null point because of the self-contained DC component during the optical modulation.

A laser with the center frequency of 193.1 THz (f_c) and a linewidth of 100 kHz is employed as the light source. Especially for OCA-SSB, an additional laser with the same frequency offset with the VCA-SSB is employed to generate the optical carrier in Fig. 3. The SSMF has the dispersion coefficient of 17 ps/nm/km and an attenuation coefficient of 0.2 dB/km. Besides, the nonlinearity of the fiber is neglected. Here we add a variable optical attenuator (VOA) to set different OSNRs as shown in Fig. 3. An erbium-doped fiber amplifier (EDFA) is utilized with the ASE noise figure of 5dB and launch power of 1 mW. At the receiver, a 5-order
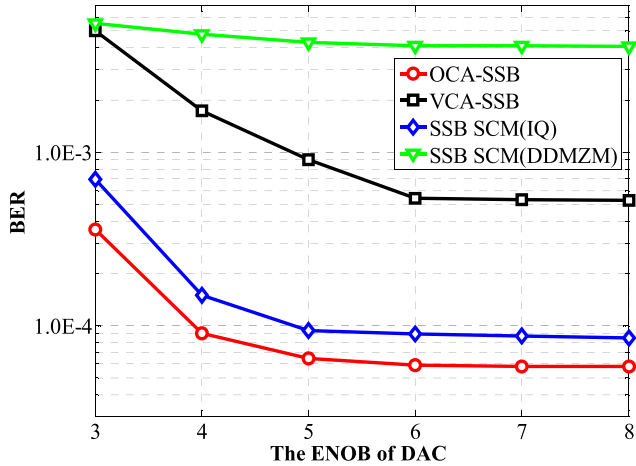
FIGURE 4. BER versus DAC ENOB for four SSB systems in back-to-back scenario.

Gaussian-shape optical band-pass filter (OBPF) with bandwidth of 65 GHz is used to remove the out-of-band optical noise. The optically filtered signal is then detected by a PIN photodiode with responsivity of 0.65 A/W. Then, the received electrical signal is further processed via Matlab. The sampling rate and the effective number of bits (ENOB) of DAC are 112 GSa/s and 6 bits, respectively.

The Rx DSP includes signal resampling, KK scheme, down conversion, CD compensation, time domain equalization, BPS algorithm, QAM demodulation and BER counting as shown in Fig. 3. Due to unwanted spectral broadening induced by nonlinear operations in the KK algorithm [41], [43], such as the logarithm and square root operation, the received signal is all up-sampled to 4 times per symbol before KK receiver.

IV. RESULTS AND DISCUSSION

We first optimize the ENOB of DAC for four SSB systems in back-to-back (BtB) scenario at a OSNR of 34 dB and launch power of 1 mW under each respective optimum CSPRs in Fig. 4, which are 9dB, 8dB, 8.5dB and 11dB for scheme (a)-(d). When the ENOB $\geq$ 6 bits, the BER performance tends to be stable for all the SSB generation schemes. In particular VCA-SSB can be observed as the most sensitive scheme to ENOB, mainly because the digital carrier added to the Tx can compress the quantization interval of the effective signal. Besides, we can see the BER curve of SSB SCM with DDMZM is above the others' due to a large DC component included in the output of DDMZM according to Eq. (10). Since higher CSPR lead to higher OSNR penalty, ASE noise is the dominant factor at a low OSNR like 34 dB and hence the influence of ENOB is not so such obvious. Although not so obvious as the other three schemes in Fig. 4, the BER curve almost tends to be stable from ENOB $\geq$ 6. As a result, the ENOB of 6 bits is employed in the followings.

Since the carrier of SSB SCM with IQM is induced by offsetting the bias of IQM, the CSPR is closely related to the parameter of the modulator, V_{bias}, which can also be
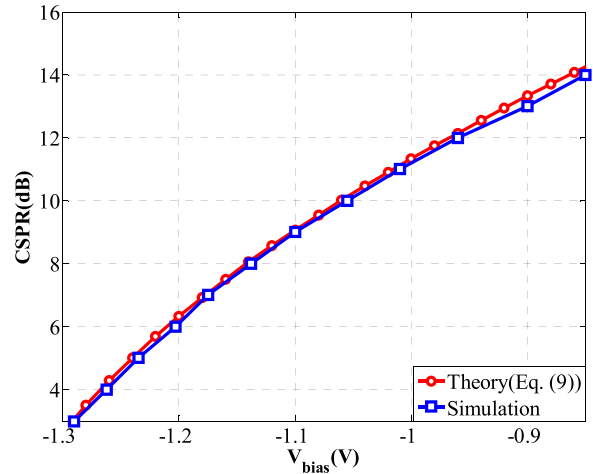

FIGURE 5. Theoretical and simulated CSPR versus V_{bias} for SSB SCM with IQM.
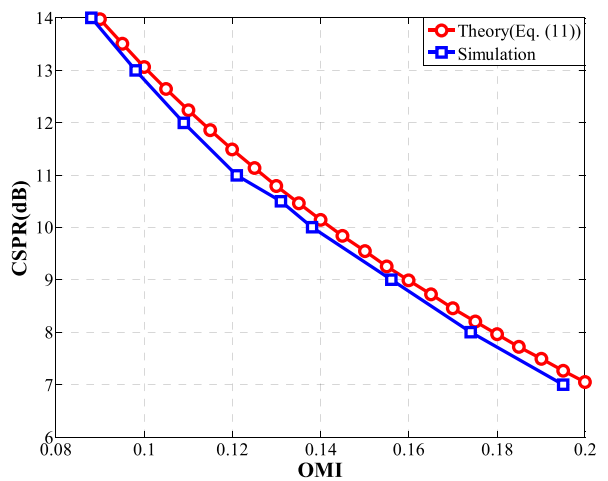

FIGURE 6. Theoretical and simulated CSPR versus *OMI* for SSB SCM with DDMZM.

concluded in Eq. (9). Therefore we compare their relationships respectively in the term of theory (according to Eq. (9)) and simulation for SSB SCM system with IQM, as shown in Fig. 5. In particular, V_{bias} here is a negative value from the setting of the formula and increases form $-V_\pi/2$ (-1.5 V in this paper). In Fig. 5, two curves fit well and the CSPR will increase as V_{bias} increases, which proves that the influence of high-order terms in Eq. (7) can be negligible on the condition of relatively small signal. Through this, we can directly figure out the best V_{bias} of IQ modulator consistent with the optimum CSPR theoretically instead of the simulation or experiment.

Similarly, Fig. 6 shows the relationship between *OMI* and the CSPR in terms of theory (according to Eq. (11)) and simulation for SSB SCM (DDMZM) system. According to Eq. (11), the CSPR of SSB SCM (DDMZM) method is only related to *OMI*. The two curves are highly closed and share the same trend that the CSPR decreases as *OMI* increases, which also proves the correctness of Eq. (11). As a result,
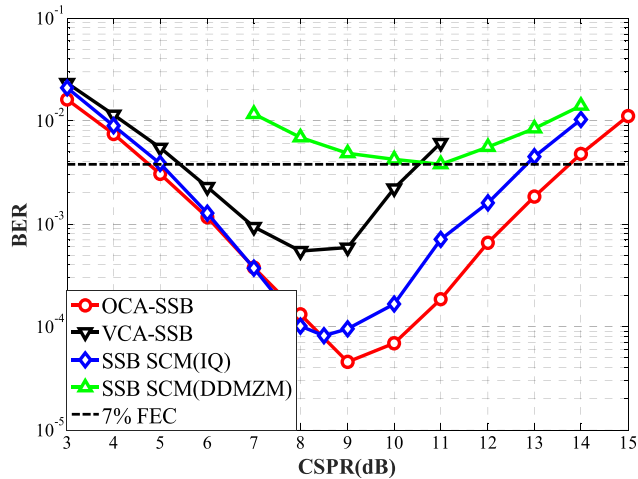
FIGURE 7. BER versus CSPR for four SSB systems at OSNR of 34 dB in back-to-back scenario.

FIGURE 8. BER versus OSNR for four SSB systems under the respective best CSPRs in back-to-back scenario.

the best value of *OMI* corresponding to the optimum CSPR in this SSB scheme, can also be acquired straightly through the conclusion in theory without any complicate experiments.

Optical CSPR is an important parameter in SSB DD systems based on KK algorithm. Fig.7 shows the BER performance versus the CSPR of four SSB systems in back-to-back (BtB) scenario. For fairly comparison, all the simulations operate at the OSNR of 34 dB. The four optimum CSPRs can be observed to be 9 dB for OCA-SSB, 8 dB for VCA-SSB, 8.5 dB for SSB SCM (IQ) and 11 dB for SSB SCM (DDMZM).

Firstly, at a fixed OSNR of 34dB, the trade-off of CSPR shown in Fig. 7 clearly divides the graph into two parts, the nonlinear and linear religion. Signals operating at lower CSPRs suffer from a large nonlinear penalty, since the minimum phase condition hasn't been met yet, while higher CSPRs lead to higher linear penalty (increased carrier-ASE beating). Secondly, in terms of different optimum CSPRs for four SSB schemes, there is not much difference between the former three systems, but the CSPR of SSB SCM (DDMZM) is almost 3 dB larger than the others'. Due to a large DC component concluded in the output of DDMZM (Eq. (10)), the CSPR inevitably becomes large, and thus the effective OSNR ($OSNR_{equivalent}$) will be relatively small, which leads to system performance degradation. As the CSPR decrease, the BER of SSB SCM (DDMZM) doesn't improve a lot mainly because the amplitude of signal becomes large enough to enter the nonlinear region of the modulator. Due to the above, the system performance of the SSB SCM (DDMZM) in this paper can hardly reach the BER of the 7% hard-decision forward error (HD-FEC) at OSNR of 34dB, as is shown in Fig.4, Fig.7 and the following figures. In addition, if we change the modulator with a smaller V_π, the system performance will be predictably better. Thirdly, we also notice the BER performance difference between four SSB schemes. With respect to VCA system, because of the limited ENOB
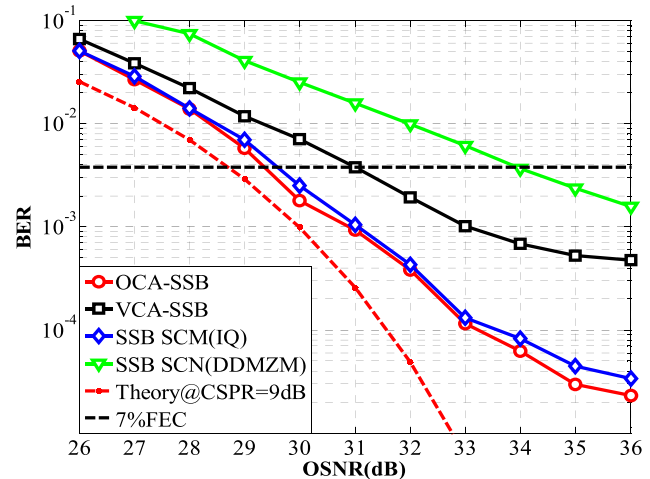
of the DACs in VCA-SSB, when the CSPR becomes large as the power of virtual carrier increases, the quantization noise will increase under the fixed quantization bit of 6 in the simulation. Therefore, the VCA-SSB system has relatively poor performance in comparison with OCA-SSB. Besides, as we mentioned in Section II, the IQM in SSB SCM systems is biased above or below the null-point to induce the optical carrier. Therefore, the symmetrical modulation curve of modulator will move up, causing a small part of the signal to enter into nonlinear region, which is the reason why the performance of OCA-SSB is better than SSB SCM with IQM.

As shown in Fig. 8, we also investigate the BER performance versus OSNR under their respective best CSPRs in back-to-back (BtB) scenario for four SSB techniques. As it appears from Fig. 8, the OSNRs required for operation at 7% FEC (corresponds to a BER of 3.8×10^{-3}) are approximately 29.4 dB for OCA-SSB (red line), 29.6 dB for VCA-SSB (black line), 31 dB for SSB SCM with IQM (blue line) and 34 dB for SSB SCM with DDMZM (green line). We can find the OSNR for OCA-SSB and SSB SCM (IQ) is just about 0.5 dB larger than the theoretical value. The OSNR penalty of VCA-SSB is mainly for the quantization noise induced by infinite ENOB of the DACs [36]. As discussed in the Fig. 7, the penalty of SSB SCM (DDMZM) can be contributed to *OMI* parameter according to Eq. (11) and nonlinearity of modulation region.

The BER performance versus the CSPR of four SSB systems after 80 km SSMF transmission is depicted in Fig. 9. For a fair comparison, we also carry out the implementation of the simulation at the OSNR of 34 dB. In contrast to Fig. 7, it is worth noting that the optimum values of CSPR all increase by about 1dB, which are 10 dB for OCA-SSB, 9.5 dB for VCA-SSB, 9 dB for SSB SCM (IQ) and 12 dB for SSB SCM (DDMZM).

As is mentioned in [29], the KK receiver can be relatively sensitive to CD, which causes signal distortion to produce the high peak-to-average power ratio (PAPR). The trajectory
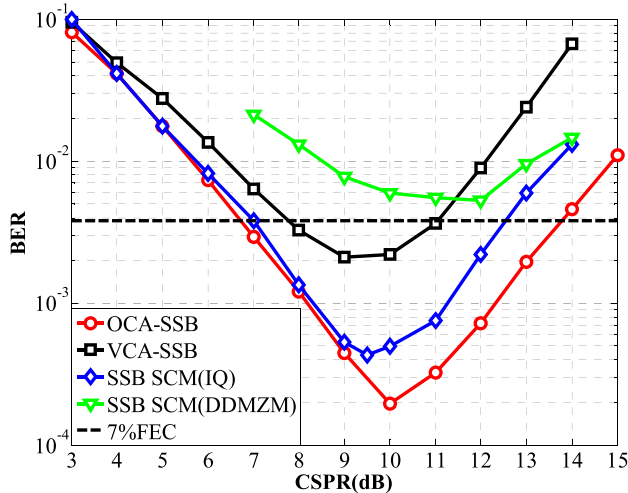
FIGURE 9. BER versus CSPR for four SSB systems at OSNR of 34 dB after 80 km SSMF transmission.
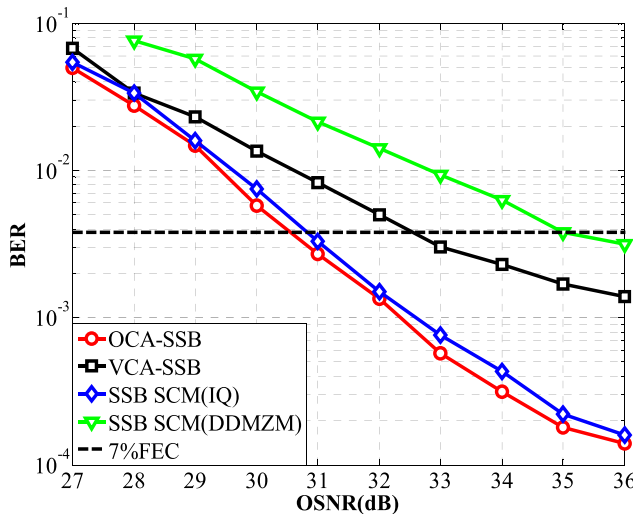

FIGURE 10. BER versus OSNR for four SSB systems under the respective best CSPRs after 80 km SSMF transmission.

of signals with high PAPR are more likely to include the origin of the complex plane [36], [41], namely, minimum phase condition is violated. Therefore, after transmission KK receiver requires a higher CSPR to be robust against CD than that used in the BtB case [44]. Thus we can observe that four curves share two same trends as the BtB scenario: the CSPR of first three methods can be considered almost the same and the last method is also 3dB larger; the BER performance of OCA-SSB and SSB SCM (IQ) outperform the remaining two techniques.

Correspondingly, we also investigate the BER performance versus the OSNR of four SSB systems after 80 km SSMF transmission in Fig. 10. Similarly, it is conducted under their respective best CSPRs of 80 km transmission. Compared to the BtB case, the OSNR penalty at 7% FEC can be observed as 30.5 dB, 30.7 dB, 32.5 dB and 35 dB respectively. Since the SSB system have a good resistance to dispersion, it is foreseeable that there's only

a marginal difference between the BtB and 80 km case. Fig. 10 shows the differences between the two cases are 1.1 dB, 1.1 dB, 1.5 dB and 1 dB respectively. As mentioned above, the OSNR penalty of 1dB is mostly attributed to the increase of optimum CSPR induced by CD, which is also 1 dB larger than BtB scenario. Furthermore, as shown in Fig. 2, it is also compatible with simulation that 1 dB increase of CSPR will bring approximately 1 dB penalty of OSNR at 7% FEC within a certain range of 6 dB to 12 dB theoretically.

V. CONCLUSION

In this paper, the theoretical derivations of SSB modulation processing and calculation formulas of carrier-signal power ratio have been given in detail based on four kinds of SSB generation schemes. It is very noteworthy that the theoretical derivations have been well consistent with the numerical analysis of simulation. Therefore, the system parameter configuration related to the CSPR can be directly confirmed without the experimental measurements in SSB-based KK systems. Besides, we also investigate the CSPR and OSNR of four SSB systems in the 224-Gb/s DD transmission over 80-km SSMF with SSB 16-QAM signal. As in BtB case, the optimum CSPRs are 9 dB for OCA-SSB, 8 dB for VCA-SSB, 8.5 dB for SSB SCM (IQ) and 11 dB for SSB SCM (DDMZM) and the OSNR penalty at 7% FEC are 29.4 dB, 29.6 dB, 31 dB. After 80 km transmission the optimum CSPRs have both increased by 1 dB due to the CD and the OSNR penalty has also increased by approximately 1 dB. The results show that within a unified optical transmission platform, the former three SSB systems share the same level of CSPRs and the system performance of OCA-SSB and SSB SCM (IQ) outperform the other two schemes. As a result, this paper can offer a theory instruction of device parameter configuration corresponding to the CSPR, which can achieve the high-performance optical transmission for low-cost metro networks.

REFERENCES

[1] K. Zhong, X. Zhou, J. Huo, C. Yu, C. Lu, and A. P. T. Lau, "Digital signal processing for short-reach optical communications: A review of current technologies and future trends," *J. Lightw. Technol.*, vol. 36, no. 2, pp. 377–400, Jan. 15, 2018.

[2] M. Ruffini *et al.*, "Access and metro network convergence for flexible end-to-end network design," *IEEE/OSA J. Opt. Commun. Netw.*, vol. 9, no. 6, pp. 524–535, Jun. 2017.

[3] K. Zhong, X. Zhou, T. Gui, L. Tao, Y. Gao, W. Chen, J. Man, L. Zeng, A. P. T. Lau, and C. Lu, "Experimental study of PAM-4, CAP-16, and DMT for 100 Gb/s short reach optical transmission systems," *Opt. Express*, vol. 23, no. 2, pp. 1176–1189, 2015.

[4] X. Xu, E. Zhou, G. N. Liu, T. Zuo, Q. Zhong, L. Zhang, Y. Bao, X. Zhang, J. Li, and Z. Li, "Advanced modulation formats for 400-Gbps short-reach optical inter-connection," *Opt. Express*, vol. 23, no. 1, pp. 492–500, Jan. 2015.

[5] Y. Zhu, X. Ruan, K. Zou, and F. Zhang, "Beyond 200G direct detection transmission with Nyquist asymmetric twin-SSB signal at C-band," *J. Lightw. Technol.*, vol. 35, no. 17, pp. 3629–3636, Sep. 1, 2017.

[6] Y. Zhu, M. Jiang, and F. Zhang, "Direct detection of polarization multiplexed single sideband signals with orthogonal offset carriers," *Opt. Express*, vol. 26, no. 12, pp. 15887–15898, Jun. 2018.

[7] X. Zhou, X. Yang, R. Li, and K. Long, "Efficient joint carrier frequency offset and phase noise compensation scheme for high-speed coherent optical OFDM systems," *J. Lightw. Technol.*, vol. 31, no. 11, pp. 1755–1761, Jun. 1, 2013.

[8] X. Zhou, J. Huo, K. Zhong, F. N. Khan, T. Gui, H. Zhang, J. Tu, J. Yuan, K. Long, C. Yu, A. P. T. Lau, and C. Lu, "Single channel 50 Gbit/s transmission over 40 km SSMF without optical amplification and in-line dispersion compensation using a single-end PD-based PDM-SSB-DMT system," *IEEE Photon. J.*, vol. 9, no. 5, Oct. 2017, Art. no. 7906911.

[9] L. Tao, Y. Wang, Y. Gao, A. P. T. Lau, N. Chi, and C. Lu, "Experimental demonstration of 10 Gb/s multi-level carrier-less amplitude and phase modulation for short range optical communication systems," *Opt. Express*, vol. 21, no. 5, pp. 6459–6465, Mar. 2013.

[10] L. Tao, Y. Wang, Y. Gao, and N. Chi, "High order CAP system using DML for short reach optical communications," *IEEE Photon. Technol. Lett.*, vol. 26, no. 13, pp. 1348–1351, Jul. 1, 2014.

[11] M. I. Olmedo, T. Zuo, J. B. Jensen, Q. Zhong, X. Xu, S. Popov, and I. T. Monroy, "Multiband carrierless amplitude phase modulation for high capacity optical data links," *J. Lightw. Technol.*, vol. 32, no. 4, pp. 798–804, Feb. 15, 2014.

[12] A. Aimone, I. G. Lopez, S. Alreesh, P. Rito, T. Brast, V. Höhns, G. Fiol, M. Gruner, J. K. Fischer, J. Honecker, A. G. Steffan, D. Kissinger, A. C. Ulusoy, and M. Schell, "DAC-free ultra-low-power dual-polarization 64-QAM transmission with InP IQ segmented MZM module," in *Proc. OFC*, Anaheim, CA, USA, Mar. 2016, Paper Th5C-6.

[13] Y. Zhu, X. Ruan, Z. Chen, M. Jiang, K. Zou, C. Li, and F. Zhang, "4×200Gb/s twin-SSB Nyquist subcarrier modulation WDM transmission over 160km SSMF with direct detection," in *Proc. OFC*, Los Angeles, CA, USA, Mar. 2017, pp. 1–3, Paper Tu3L.2.

[14] J. L. Wei, J. D. Ingham, Q. Cheng, D. G. Cunningham, R. V. Penty, and I. H. White, "Experimental demonstration of optical data links using a hybrid CAP/QAM modulation scheme," *Opt. Lett.*, vol. 39, no. 6, pp. 1402–1405, Mar. 2014.

[15] X. Zhou, "An improved feed-forward carrier recovery algorithm for coherent receivers with *M*-QAM modulation format," *IEEE Photon. Technol. Lett.*, vol. 22, no. 14, pp. 1051–1053, Jul. 15, 2010.

[16] X. Ruan, K. Li, D. J. Thomson, C. Lacava, F. Meng, I. Demirtzioglou, P. Petropoulos, Y. Zhu, G. T. Reed, and F. Zhang, "Experimental comparison of direct detection Nyquist SSB transmission based on silicon dual-drive and IQ Mach–Zehnder modulators with electrical packaging," *Opt. Express*, vol. 25, no. 16, pp. 19332–19342, Aug. 2017.

[17] Y. Zhu, M. Jiang, X. Ruan, Z. Chen, C. Li, and F. Zhang, "6.4 Tb/s (32×200 Gb/s) WDM direct-detection transmission with twin-SSB modulation and Kramers–Kronig receiver," *Opt. Commun.*, vol. 415, pp. 64–69, May 2018.

[18] M. S. Erkılınç, S. Pachnicke, H. Griesser, B. C. Thomsen, P. Bayvel, and R. I. Killey, "Performance comparison of single-sideband direct detection Nyquist-subcarrier modulation and OFDM," *J. Lightw. Technol.*, vol. 33, no. 10, pp. 2038–2046, May 15, 2015.

[19] X. Ruan, L. Zhang, F. Yang, Y. Zhu, Y. Li, and F. Zhang, "Beyond 100G single sideband PAM-4 transmission with silicon dual-drive MZM," *IEEE Photon. Technol. Lett.*, vol. 31, no. 7, pp. 509–512, Apr. 1, 2019.

[20] J. Huo, X. Zhou, K. Zhong, J. Tu, W. Huangfu, J. Yuan, Z. Kang, K. Long, C. Yu, A. P. T. Lau, and C. Lu, "Experimental study of single channel 100 Gbit/s PAM4 transmission over 40 km using 17 GHz EML and APD at O band," *Opt. Fiber Technol.*, vol. 45, pp. 411–414, Nov. 2018.

[21] J. Huo, X. Zhou, K. P. Zhong, J. Tu, J. Yuan, C. Guo, K. Long, C. Yu, A. P. T. Lau, and C. Lu, "Transmitter and receiver DSP for 112 Gbit/s PAM-4 amplifier-less transmissions using 25G-class EML and APD," *Opt. Express*, vol. 26, no. 18, pp. 22673–22686, Sep. 2018.

[22] R. Rath, D. Clausen, S. Ohlendorf, S. Pachnicke, and W. Rosenkranz, "Tomlinson–Harashima precoding for dispersion uncompensated PAM-4 transmission with direct-detection," *J. Lightw. Technol.*, vol. 35, no. 18, pp. 3909–3917, Sep. 15, 2017.

[23] N. Cvijetic, "OFDM for next-generation optical access networks," *J. Lightw. Technol.*, vol. 30, no. 4, pp. 384–398, Feb. 15, 2012.

[24] B. Schmidt, A. J. Lowery, and J. Armstrong, "Experimental demonstrations of electronic dispersion compensation for long-haul transmission using direct-detection optical OFDM," *J. Lightw. Technol.*, vol. 26, no. 1, pp. 196–203, Jan. 1, 2008.

[25] M. Schuster, S. Randel, C. A. Bunge, S. C. J. Lee, F. Breyer, B. Spinnler, and K. Petermann, "Spectrally efficient compatible single-sideband modulation for OFDM transmission with direct detection," *IEEE Photon. Technol. Lett.*, vol. 20, no. 9, pp. 670–672, May 1, 2008.

[26] T. M. F. Alves and V. T. Cartaxo, "Performance comparison of power fading mitigation techniques in multiband OFDM-UWB signals transmission along LR-PONs," *Chin. Opt. Lett.*, vol. 11, no. 8, pp. 080602-1–080602-6, Aug. 2013.

[27] M. S. Erkılınç, Z. Li, S. Pachnicke, H. Griesser, B. C. Thomsen, P. Bayvel, and R. I. Killey, "Spectrally efficient WDM Nyquist pulse-shaped 16-QAM subcarrier modulation transmission with direct detection," *J. Lightw. Technol.*, vol. 33, no. 15, pp. 3147–3155, Aug. 1, 2015.

[28] Y. Zhu, K. Zou, Z. Chen, and F. Zhang, "224 Gb/s optical carrier-assisted Nyquist 16-QAM half-cycle single-sideband direct detection transmission over 160 km SSMF," *J. Lightw. Technol.*, vol. 35, no. 9, pp. 1557–1565, May 1, 2017.

[29] C. Sun, D. Che, and W. Shieh, "Comparison of chromatic dispersion sensitivity between Kramers–Kronig and SSBI iterative cancellation receiver," in *Proc. OFC*, San Diego, CA, USA, Mar. 2018, Paper W4E.4.

[30] B. J. C. Schmidt, Z. Zan, L. B. Du, and A. J. Lowery, "120 Gbit/s over 500-km using single-band polarization-multiplexed self-coherent optical OFDM," *J. Lightw. Technol.*, vol. 28, no. 4, pp. 328–335, Feb. 15, 2010.

[31] W.-R. Peng, X. Wu, V. R. Arbab, K.-M. Feng, B. Shamee, L. C. Christen, J.-Y. Yang, A. E. Willner, and S. Chi, "Theoretical and experimental investigations of direct-detected RF-tone-assisted optical OFDM systems," *J. Lightw. Technol.*, vol. 27, no. 10, pp. 1332–1339, May 15, 2009.

[32] C. Ju, X. Chen, and N. Liu, "Subcarriers-to-subcarriers beating interference cancellation in virtual single sideband optical frequency division multiplexing system," *Opt. Eng.*, vol. 53, no. 9, Sep. 2014, Art. no. 096110.

[33] M. S. Erkılınç, M. P. Thakur, S. Pachnicke, H. Griesser, J. Mitchell, B. C. Thomsen, P. Bayvel, and R. I. Killey, "Spectrally efficient WDM Nyquist pulse-shaped subcarrier modulation using a dual-drive Mach–Zehnder modulator and direct detection," *J. Lightw. Technol.*, vol. 34, no. 4, pp. 1158–1165, Feb. 15, 2016.

[34] Z. Li, M. S. Erkılınç, K. Shi, E. Sillekens, L. Galdino, T. Xu, B. C. Thomsen, P. Bayvel, and R. I. Killey, "Spectrally efficient 168 Gb/s/λ WDM 64-QAM single-sideband Nyquist-subcarrier modulation with Kramers–Kronig direct-detection receivers," *J. Lightw. Technol.*, vol. 36, no. 6, pp. 1340–1346, Mar. 15, 2018.

[35] X. Zhang, C. Zhang, C. Chen, W. Jin, X. Zhong, and K. Qiu, "Digital chromatic dispersion pre-management for SSB modulation direct-detection optical transmission systems," *Opt. Commun.*, vol. 427, pp. 551–556, Nov. 2018.

[36] S. T. Le, K. Schuh, M. Chagnon, F. Buchali, R. Dischler, V. Aref, H. Buelow, and K. M. Engenhardt, "1.72-Tb/s virtual-carrier-assisted direct-detection transmission over 200 km," *J. Lightw. Technol.*, vol. 36, no. 6, pp. 1347–1353, Mar. 15, 2018.

[37] S. Randel, D. Pilori, S. Chandrasekhar, G. Raybon, and P. Winzer, "100-Gb/s discrete-multitone transmission over 80-km SSMF using single-sideband modulation with novel interference-cancellation scheme," in *Proc. ECOC*, Valencia, Spain, Sep./Oct. 2015, pp. 1–3, Paper Mo4.5.2.

[38] W.-R. Peng, B. Zhang, K.-M. Feng, X. Wu, A. E. Willner, and S. Chi, "Spectrally efficient direct-detected OFDM transmission incorporating a tunable frequency gap and an iterative detection techniques," *J. Lightw. Technol.*, vol. 27, no. 24, pp. 5723–5735, Dec. 15, 2009.

[39] Z. Li, M. S. Erkılınç, R. Maher, L. Galdino, K. Shi, B. C. Thomsen, P. Bayvel, and R. I. Killey, "Two-stage linearization filter for direct-detection subcarrier modulation," *IEEE Photon. Technol. Lett.*, vol. 28, no. 24, pp. 2838–2841, Dec. 15, 2016.

[40] Z. Li, M. S. Erkilinc, R. Maher, L. Galdino, K. Shi, B. C. Thomsen, B. Bayvel, and R. I. Killey, "Reach enhancement for WDM direct-detection subcarrier modulation using low-complexity two-stage signal-signal beat interference cancellation," in *Proc. ECOC*, Dusseldorf, Germany, Sep. 2016, pp. 1–3, Paper M.2.B.1.

[41] A. Mecozzi, "Kramers–Kronig coherent receiver," *Optica*, vol. 3, no. 11, pp. 1220–1227 , Jun. 2016.

[42] Z. Li, M. S. Erkilinc, L. Galdino, K. Shi, B. C. Thomsen, P. Bayvel, and R. I. Killey, "Comparison of digital signal-signal beat interference compensation techniques in direct-detection subcarrier modulation systems," *Opt. Express*, vol. 24, no. 25, pp. 29176–29189, Dec. 2016.

[43] Z. Li, M. S. Erkilinç, K. Shi, E. Sillekens, L. Galdino, B. C. Thomsen, P. Bayvel, and R. I. Killey, "SSBI mitigation and the Kramers–Kronig scheme in single-sideband direct-detection transmission with receiver-based electronic dispersion compensation," *J. Lightw. Technol.*, vol. 35, no.10, pp. 1887–1893, May 15, 2017.

[44] A. Mecozzi, "A necessary and sufficient condition for minimum phase and implications for phase retrieval," Jun. 2016, *arXiv:1606.04861*. [Online]. Available: https://arxiv.org/abs/1606.04861

[45] Q. Zhang, N. Stojanovic, C. Xie, C. Prodaniuc, and P. Laskowski, "Transmission of single lane 128 Gbit/s PAM-4 signals over an 80 km SSMF link, enabled by DDMZM aided dispersion pre-compensation," *Opt. Express*, vol. 24, no. 21, pp. 24580–24591, Oct. 2016.

DONGXU LU was born in Shandong, China, 1991. He received the B.S. degree in electronic science and technology from Xidian University, Xi'an, Shanxi, in 2012. He is currently pursuing the Ph.D. degree in information and communication engineering with the University of Science and Technology Beijing (USTB). His main research interests include short reach optical transmission systems, optical interconnect, and signal processing.
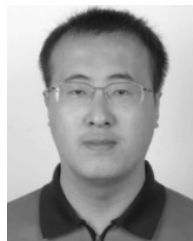
XIAN ZHOU received the Ph.D. degree in electromagnetic field and microwave techniques from the Beijing University of Posts and Telecommunications, China, in 2011. She was a Postdoctoral Fellow with the Department of Electrical and Information Engineering, The Hong Kong Polytechnic University, from February 2014 to February 2017. She is currently a Professor with the School of Computer and Comm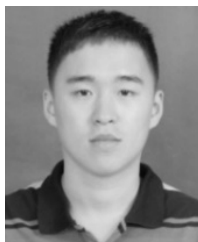unication Engineering, University of Science and Technology Beijing. Her current research interests include system designs and signal processing techniques for coherent fiber-optic communication systems, and short reach optical communications.

JIAHAO HUO was born in Hebei, China, 1989. He received the M.S. degree from the Changchun University of Science and Technology, in June 2014, the Ph.D. degree from the University of Science and Technology Beijing, in 2019. He joined the Photonics Research Center, The Hong Kong Polytechnic University, in June 2016, as a Research Assistant. He is currently a Lecturer with the University of Science and Technology Beijing. His research interests include high-capacity IM/DD systems for optical interconnect, optical access networks, and digital signal processing techniques for advanced modulation formats.

JIE GAO was born in Henan, China, 1994. She is currently pursuing the master's degree in information and communication engineering with the University of Science and Technology Beijing (USTB). Her main research interests include machine learning and modulation format identification in optical communication systems.

YUQIANG YANG was born in Hebei, China, 1994. He is currently pursuing the master's degree in information and communication engineering with the University of Science and Technology Beijing (USTB). His main research interests include short reach optical transmission systems, optical modulation, and signal processing.

KE HE received the Ph.D. degree in communication and information systems from the Beijing University of Posts and Telecommunications, China, in 2012. He is currently working with the University of Science and Technology Beijing and the Sichuan Energy Internet Research Institute. His research interest includes integration of optical and wireless access networks.

JINHUI YUAN received the B.S. and M.S. degrees from Yanshan University, Qinhuangdao, China, in 2005 and 2008, respectively, and the Ph.D. degree from the Beijing University of Posts and Telecommunications (BUPT), Beijing, China, in 2011. He was an Associate Professor with BUPT. He is currently a Professor with the University of Science and Technology Beijing. He is also a Hong Kong Scholar with the Photonics Research Centre, Department of Electronic and Information Engineering, The Hong Kong Polytechnic University. He has published more than 100 articles in the academic journals and conferences. His current research interests include photonic crystal fibers, silicon waveguide, and optical fiber devices. He is also a member of OSA.

KEPING LONG received the M.S. and Ph.D. degrees in electric circuit and systematic from the University of Electronic Science and Technology of China (UESTC), Chengdu, China, in 1995 and 1998, respectively. He is currently a Full Professor and the Dean of the School of Computer and Communication Engineering, University of Science and Technology Beijing. His main research interests include optical internet and switching technology, cooperative communications, and computer networks.
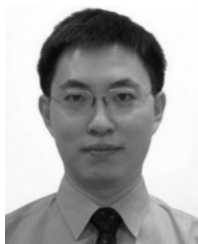
CHANGYUAN YU received the Ph.D. degree in electrical engineering from the University of Southern California, USA, in 2005. He was a Visiting Researcher with NEC Labs America in Princeton, USA, in 2005. He then joined the Faculty of National University of Singapore, in 2005. He served as the Founding Leader of the Photonic System Research Group, Department of Electrical and Computer Engineering. He was also a Joint Senior Scientist with the A*STAR Institute for Infocomm Research, Singapore. In 2015, he joined the Department of Electronic and Information Engineering, The Hong Kong Polytechnic University as an Associate Professor. His research focuses on photonic devices, subsystems, optical fiber communication and sensor systems, and medical instruments. He has coauthored six book chapters and 360 journal and conference papers (66 invited, including OFC2012, USA). He has served in technical program committee (TPC) or organizing committee for over 80 international conferences, including a TPC Member of OFC, from 2014 to 2016, a TPC Chair of SPPCom 2014 and OECC 2017, and a General Chair of SPPCom 2016 and 2015. His group won six best paper awards in conferences and the championship in biomedical area in the 3rd China Innovation and Entrepreneurship Competition (out of over 10,000 competitors), in 2014.

ALAN PAK TAO LAU received the B.A.Sc. degree in engineering science (electrical option) and the M.A.Sc. degree in electrical and computer engineering from the University of Toronto, in 2003 and 2004, respectively, and the Ph.D. degree in electrical engineering with Stanford University, in 2008. He joined The Hong Kong Polytechnic University as an Assistant Professor.

In summer 2006, he worked with NEC Labs America, on receiver structures for multimode fiber systems. He is currently an Associate Professor. His current research interests include long-haul and short-reach coherent optical communication systems, optical performance monitoring, and machine learning applications in optical communications and networks. He collaborates extensively with industry. He is also the Principle Investigator of various governmental- and industry-funded research projects in various aspects of optical communications. He serves on technical program committees for international conferences in the areas of photonics and communications.

CHAO LU received the B.Eng. degree in electronic engineering from Tsinghua University, China, in 1985, and the M.Sc. and Ph.D. degrees from the University of Manchester, U.K., in 1987 and 1990, respectively. He joined the School of Electrical and Electronic Engineering, Nanyang Technological University, Singapore, as a Lecturer, in 1991. He has been an Associate Professor, since January 1999. From June 2002 to December 2005, he was seconded to the Institute for Infocomm Research, Agency for Science, Technology and Research (A*STAR), Singapore, as a Program Director and the Department Manager, where he was helping to establish a Research Group in the area of optical communication and fiber devices. Since April 2006, he has been a Professor with the Department of Electronic and Information Engineering, The Hong Kong Polytechnic University. His research interests are optical communication systems and networks, and fiber devices for optical communication and sensor systems.

● ● ●